JTTEE5 9:38-48

Thermal Cycling Behavior of Plasma-Sprayed Thermal Barrier Coatings with Various MCrAlX Bond Coats

J.A. Haynes, M.K. Ferber, and W.D. Porter

(Submitted 26 January 1999; in revised form 5 December 1999)

The influence of bond coat composition on the spallation resistance of plasma-sprayed thermal barrier coatings (TBCs) on single-crystal René N5 substrates was assessed by furnace thermal cycle testing of TBCs with various vacuum plasma spray (VPS) or air plasma-spray (APS) MCrAlX (M = Ni and/or Co; and X = Y, Hf, and/or Si) bond coats. The TBC specimens with VPS bond coats were fabricated using identical parameters, with the exception of bond coat composition. The TBC lifetimes were compared with respect to MCrAlX composition (before and after oxidation testing) and MCrAlX properties (surface roughness, thermal expansion, hardness, and Young's modulus). The average TBC spallation lifetimes varied significantly (from 174 to 344 1 h cycles at 1150 °C) as a function of bond coat composition. Results suggested a relationship between TBC durability and bond coat thermal expansion behavior below 900 °C. Although there were only slight differences in their relative rates of cyclic oxidation weight gain, VPS MCrAlX bond coats with better oxide scale adhesion provided superior TBC lifetimes.

Keywords TBCs, thermal barrier coatings, cyclic oxidation, plasma spray, bond coat

1. Introduction

There is significant interest in developing an improved understanding of the degradation mechanisms of plasma-sprayed thermal barrier coatings (TBCs) systems, so that coatings with improved performance can be designed. Bilayer plasma-sprayed TBCs, which consist of an oxidation-resistant metallic bond coat overlaid with a thermally insulating ceramic top coat, are commonly used to protect stationary, hot-section superalloy components in gas turbine engines.[1] The porous ceramic top coat, which is typically 6 to 8 wt.% Y_2O_3-stabilized ZrO_2 (YSZ), protects the underlying air-cooled engine component by significantly reducing its operating temperature.[1,2] However, the reliability and durability of plasma-sprayed TBCs are limited by the tendency of the ceramic top coat to prematurely fracture and spall during thermal cycling. Although various types of plasma-sprayed TBCs have been in commercial engine service on stationary components for at least 3 decades,[3] there is still an inadequate understanding of their specific degradation mechanisms,[4,5] which limits efforts to significantly improve TBC design and life prediction capabilities.

The metallic bond coat plays a critical role in TBC performance, since it provides both oxidation resistance and a surface to which the plasma-sprayed YSZ can physically and/or chemically bond. The bond coat may also serve as a compliant layer (at high temperatures) that partially accommodates thermal stresses. Bond coats for plasma-sprayed TBCs typically consist of a variety of MCrAlX alloys, where M = Ni and/or Co and X = Y, Hf, and/or Si. These MCrAlX alloys are applied to the superalloy surface by either air plasma-spray (APS), which results in a porous metallic coating with moderate oxidation resistance, or by vacuum plasma-spray (VPS), which provides a bond coat with minimal porosity and superior oxidation resistance. It is commonly assumed that the rough surface of the plasma-sprayed bond coat promotes adhesion of the plasma-sprayed ceramic top coat,[1] although a rough bond coat surface may not be necessary in all cases.[6] During high-temperature exposure, a thin protective Al_2O_3 scale (which is the basis for the oxidation resistance of the bond coat) forms along the rough bond coat-YSZ interface by selective oxidation of Al in the metallic coating.

The typical failure mode of plasma-sprayed TBCs during both engine service and laboratory testing is fracture and delamination of the porous YSZ near to and parallel to the irregular bond coat interface.[1,5,7-9] Although a multitude of phenomena contribute to TBC degradation, it is generally agreed that the predominant TBC damage mechanisms are (1) YSZ residual stresses induced by metal-ceramic thermal expansion mismatch (during cooling) and (2) interfacial bond coat oxidation. Residual stresses in the ceramic layers (Al_2O_3 and YSZ) are influenced by the topology of the metal-ceramic interface,[10] the thermal expansion characteristics of the bond coat and superalloy,[11] and the constrained interfacial volume increase due to growth of the Al_2O_3 scale. Localized ceramic residual stresses, which typically consist of a combination of in-plane compression and out-of-plane tension,[12] are difficult to measure and predict due to the complexity of the interface morphology and YSZ microstructure, as well as a lack of sufficient information on time- and temperature-dependent materials properties.[5,11,13]

The oxidation behavior of the bond coat (which depends on MCrAlX composition and microstructure) is clearly an important factor, since bond coats with poor oxidation resistance result in rapid TBC failure.[1,2,3] The fracture resistance and adhesion behavior of the interfacial Al_20_3 scale may also be important

J.A. Haynes, M.K. Ferber, and **W.D. Porter,** Oak Ridge National Laboratory, Oak Ridge, TN 37831-6063.

issues,[7-9,14-16], although these topics have received relatively little attention with regard to plasma-sprayed TBCs. There is also phenomenological evidence that suggests bond coat properties such as strength and creep response exert a significant influence on TBC thermomechanical stability.[1,4,11,13]

A review of the literature indicates substantial differences in the thermal cycle lifetimes of various plasma-sprayed TBC systems.[1,4-6,8,9,14,17] Much of the variability from study to study can be attributed to differences in substrate quality, specimen geometry, powder materials, plasma-spray parameters, postdeposition residual stresses in the YSZ, test conditions, bond coat microstructure, and oxidation behavior. These differences complicate interpretation of results and often prevent definition or comparison of the dominant driving force(s) behind the failure of specific TBC systems.

The primary objective of this study was to systematically investigate the influence of bond coat composition on the spallation resistance of plasma-sprayed TBCs. In an effort to isolate the influence of bond coat composition, TBC specimens were fabricated with identical superalloy substrates, VPS bond coat deposition parameters, MCrAlX powder sizes, and APS YSZ top coats. A superalloy with excellent oxidation resistance (single-crystal René N5, provided by General Electric Aircraft Engines, Cincinnati, OH) was selected as the standard substrate, so that substrate degradation would not significantly influence the results. The thermal cycle lifetimes of the various types of TBCs were compared by furnace cycling at an elevated temperature (1150 °C) to accelerate the coating degradation process. The relative TBC lifetimes were then correlated to the MCrAlX bond coat: (1) cyclic oxidation behavior, (2) composition (as a function of time at temperature), (3) thermal expansion behavior, (4) room-temperature hardness and Young's modulus (with respect to time-at-temperature), and (5) surface roughness.

2. Materials and Experimental Methods

2.1 Materials

Superalloy substrate discs (2.2 cm diameter × 0.3175 cm thick, with 0.08 cm edge radii) were electrodischarge machined from single-crystal slabs of René N5. Table 1 shows the nominal composition of the superalloy.

All coatings in this study were fabricated at the Thermal Spray Lab at the State University of New York – Stony Brook (Stony Brook, NY). The superalloy substrate discs were grit blasted with Al_2O_3 and then plasma sprayed with MCrAlX to a nominal thickness of 125 μm. Three bond coat compositions (in wt.%) were used: Ni-22Cr-10Al-1Y, Ni-22Cr-10Al0.25Y, and Ni-22Co-18Cr-12.5A1-0.4Y-0.15Hf-0.25Si. These three alloys will be referred to as NiCrAl-1Y, NiCrAl-0.25Y, and NiCoCrA1YHfSi, respectively. The NiCrAl-1Y bond coats were applied by both APS and VPS, whereas the NiCrAl-0.25Y and NiCoCrAlYHfSi bond coats were deposited by VPS only (Table 2). All specimens were coated on only one face. Overspray from plasma spraying was removed from the substrate edges by grinding, and all exposed René N5 superalloy surfaces were ground to a 240 grit finish with SiC paper.

A single, coarse NiCrAlY powder (−106/+53 μm) was used to deposit APS NiCrAl-1Y (Table 2). All VPS bond coats were fabricated in two steps, using two different powder sizes (Table 2). The substrates were first preheated to approximately 900 °C in the vacuum chamber by a transferred arc process. A fine powder size (−45/+10 μm) was used to deposit the first 75 μm of VPS MCrAlX, in order to achieve a high-density inner layer. The coarser powder (−106/+53 μm) was then used to deposit the outer 50 μm of VPS MCrAlX, to increase the bond coat surface roughness. The two coating steps were part of a continuous process (*i.e.*, the specimens did not cool between VPS coating steps). All VPS bond coats were deposited using identical deposition parameters (*i.e.,* the processes were not optimized for the specific MCrAlX systems), and specimens were not annealed prior to oxidation testing. The APS and VPS deposition parameters for all MCrAlX coatings in this study are listed in Table 3.

Selected MCrAlX-coated substrates were overlaid with APS YSZ top coats to a nominal thickness of 250 μm. These specimens will be referred to hereafter as TBC specimens. All TBC specimens received identical APS YSZ top coats, fabricated by the same robotically controlled APS system, with back-face cooling to reduce specimen deposition temperature. The ceramic top coats consisted of 7.5 wt.% Y_2O_3-ZrO_2 (containing 1.5 wt.% HfO_2). The spherical YSZ powders were −106/+10 μm in size (204NS, Metco, Westbury, NY). The APS YSZ plasmaspray parameters are listed in Table 3. All TBC specimens were coated on one face.

2.2 Thermal Cycle Testing

In order to evaluate and compare the durability of the various TBC systems, laboratory thermal cycle testing was conducted in a programmable, automated bottom-drop furnace (CM Furnaces, Bloomfield, NJ) at 115 °C in static ambient air. Bare superalloy substrates, bare MCrA1X bond coats on substrates, and TBCs were tested. Each thermal cycle consisted of a 15 min ramp to 1150 °C (±6 °C), a 60 min isothermal hold at 1150 °C, and forced air cooling for 30 min to approximately 25 °C. The disc specimens were placed on a porous Al_2O_3 plate during cyclic testing (with coatings facing upward). Specimens were removed from the furnace, visually inspected, and weighed at 12 cycle intervals, and their positions on the test plate were rotated after each set of 12 cycles. The measured specimen weights did not include spallation products.

The TBC specimens were run to either 100 cycles or to TBC failure. Failure was defined as visible cracking of the APS YSZ (away from a specimen edge) or spallation of more than 10% of the YSZ. Specimens consisting of bare MCrAlX-bond coats on René N5 were cycled to the average lifetime of their associated TBC specimens in order to evaluate and compare MCrAlX oxide scale adhesion behavior over the same test interval.

Table 1 Nominal compositions of the superalloy substrates (wt.%)

Material	Ni	Co	Cr	Ta	Al	W	Re	Mo	Hf	Ti	Y	C
René N5	Bal	7.33	7.03	6.42	6.05	5.13	3.05	1.40	0.15	0.01	0.1	0.05

Table 2 Bond coats and MCrAlX powders

Bond coat	Superalloy substrate	Deposition process	Powder size(s)	Powder designation	Powder manufacturer
NiCrAl-1Y(a)	René N5	APS	−106/+53 μm	Ni 164/211	Praxair(b)
NiCrAl-1Y(a)	René N5	VPS	−45/+10 μm	Ni-343	Praxair(b)
			−106/+53 μm	Ni 164/211	Praxair(b)
NiCrAl-0.25Y(c)	René N5	VPS	−45/+10 μm	Ni-292-2	Praxair(b)
			−106/+53 μm	Ni-292-1	Praxair(b)
NiCoCrAlYHfSi(d)	René N5	VPS	−45/+10 μm	Ni-192-4	Praxair(b)
			−106/+53 μm	Ni-192-15	Praxair(b)

(a) NiCrAl-1Y = Ni-22Cr-10Al-1Y (wt.%). (b) Praxair Specialty Powders (Indianapolis, IN). (c) NiCrAl-0.25Y = Ni-22Cr-10Al-0.25Y (wt.%).
(d) NiCoCrAlYHfSi = Ni-22Co-18Cr-12.5Al-0.3Y-0.15Hf-0.25 Si (wt.%)

Table 3 Plasma-spray parameters for APS and VPS bond coats and APS top coats

Parameter	APS MCrAlX	VPS MCrAlX	APS YSZ
Gun type	Sulzer F4MB	Sulzer F4VB	Sulzer F4MB
Nozzle size (mm)	8	7	8
Gun amperage (amps)	500	650	500
Gun voltage (V)	67	68	71
Primary Ar (slpm)	50	50	35
Secondary H (slpm)	8.5	8.5	10
Carrier Ar (slpm)	2.5	2	2.5
Chamber pressure (mbar)	Atm	60	Atm
Spray distance (mm)	120	300	120
Gun traverse speed (mm/s)	30	30	30
Substrate rotation (rpm)	160	160	160
Powder feed rate (g/min)	40	40	35

2.3 Metallography and Characterization

After cyclic testing, TBC specimens were vacuum infiltrated by two-part epoxy, cut with a slow speed diamond saw, and mounted in epoxy. They were sequentially ground to a 600 grit (SiC) finish and automatically polished (vibratory) with 3 μm diamond paste and 0.05 μm colloidal silica. Coatings were characterized by field-emission gun-scanning electron microscopy (FEG-SEM; S800 and S4500, Hitachi, Tokyo, Japan) and energy dispersive spectroscopy.

2.4 Thermal Expansion Measurements

The thermal expansion behavior of cast Ni-20Cr-10Al-0.3Y (wt.%) and Ni-22Co-18Cr12.5Al-0.3Y alloys, as well as the René N5 superalloy, was measured to assess the relative influence of substrate and bond coat thermal expansion behavior on TBC durability. Note that there were no Hf or Si additions to the cast NiCoCrAlY alloy. The superalloy and cast MCrAlX specimens were electrodischarge machined to rods of 4 mm diameter × 10 mm length. Thermal expansion measurements were made from 25 to 1200 °C, using a Theta Industries (Port Washington, NY) dual push rod differential dilatometer. A tungsten rod with a length of 10 mm was used as the reference material. A platinum/platinum-10% rhodium type S thermocouple was used to monitor the sample temperature. The accuracy of the expansion measurements was determined to be better than ±2% over the range of 20 to 1450 °C by means of verification tests using sapphire and tungsten reference materials.

Oxidation of the samples during the dilatometer runs was minimized by evacuating the system, followed by backfilling with titanium-gettered helium (three times). During the test, a helium flow rate of 5 mL/min was maintained at a slight overpressure of 3 psi. Expansion measurements were made using a computerized data acquisition system, while the samples were heated and cooled at a rate of 3 °C/min. Data sets were stored at 30 s intervals.

2.5 Mechanical Properties Microprobe Analysis

The room-temperature mechanical properties, specifically hardness (H) and Young's modulus (E), of the MCrAlX bond coats were measured with a mechanical properties microprobe (Nano Indenter II, Nano Instruments, Oak Ridge, TN) using a Berkovich diamond indenter. The use of this technique for measurement of thin oxide scale properties has been described in detail elsewhere.[16,18] Carefully selected locations on coating metallographic cross sections were indented to a depth of 200 nm (8 to 10 indents per specimen). After testing, each indent was inspected in order to ensure correct placement. Indents whose H or E values were significantly lower than average or those that were in close proximity to a visible second phase or porosity were disregarded.

2.6 Surface Roughness Measurements

Surface roughness profiles of the four types of as-deposited bond coats (APS NiCrAl-1Y, VPS NiCrAl-1Y, VPS NiCrAl-0.25Y, and VPS NiCoCrAlYHfSi) were measured using a Rank Taylor Hobson contact profilometer (Rank Taylor Hobson Limited, Leicester, England). Three measurements of 5 mm length were made at random locations on each bond coat surface using a stylus with a 2.0 μm tip radius.

2.7 Electron Microprobe Analysis

The compositions of the various MCrAlX bond coats were measured on metallographic cross sections in the as-deposited condition, after 100 1 h cycles and after TBC failure. Quantitative compositional analysis was conducted with an electron

microprobe (JEOL Superprobe 733, Tokyo, Japan) at 20 kV. Elements were calibrated against pure standards and measured peak counts were corrected using the PRZ (Phi-Rho-Z) method. Data were collected as a line profile at 2 to 5 μm intervals across the bond coat thickness.

3. Results

Typical microstructures of as-deposited TBCs with APS and VPS bond coatings are shown in the backscattered electron (BSE) images of TBC metallographic sections in Fig.1(a) and (b), respectively. The as-deposited APS NiCrAl-1Y bond coats (Fig. 1c) contained high levels of porosity and entrained oxides, due to oxidation of Al and Y during plasma processing at atmospheric pressure. The three types of as-deposited VPS MCrAlX bond coats displayed relatively high densities and similar microstructures (Fig. 1d).

Characterization of metallographic cross sections of failed TBCs indicated similar failure modes for all TBCs in this study, regardless of bond coat composition. The observed failure mode was fracture and delamination of the YSZ layer near to, but typically above, the irregular bond coat interface, as shown in Fig. 2.

3.1 Thermal Cycle Testing of TBCs

Furnace thermal cycle testing of TBC specimens with René N5 substrates and identical APS YSZ top coats revealed significant differences in TBC lifetimes depending on the MCrAlX bond coat composition and deposition method. Figure 3 compares the average lifetimes of the TBCs in this study. The TBCs with VPS NiCrAl-1Y bond coats were the most durable and exhibited a 20% improvement in lifetime as compared to TBCs with APS NiCrAl-1Y bond coats. The lifetimes of TBCs with VPS NiCoCrAlYHfSi bond coats were ~50% lower than TBC lifetimes on VPS NiCrAl-1Y and ~37% lower than those on APS NiCrAl-1Y. The range of values in Fig. 3 indicates relatively good consistency in coating lifetimes (within the constraints of the specimen amounts).

Representative weight change curves during thermal cycle testing of the various TBC specimens on René N5 substrates are compared to bare René N5 in Fig. 4. There was little internal oxidation of the VPS bond coats or René N5 (as determined by SEM analysis of metallographic cross sections), so the weight changes of these specimens can be attributed to their relative oxidation behavior at the metal surfaces. Specimens with APS NiCrAl-1Y bond coats experienced oxidation along internal porosity, which is reflected by their higher weight gains (Fig. 4).

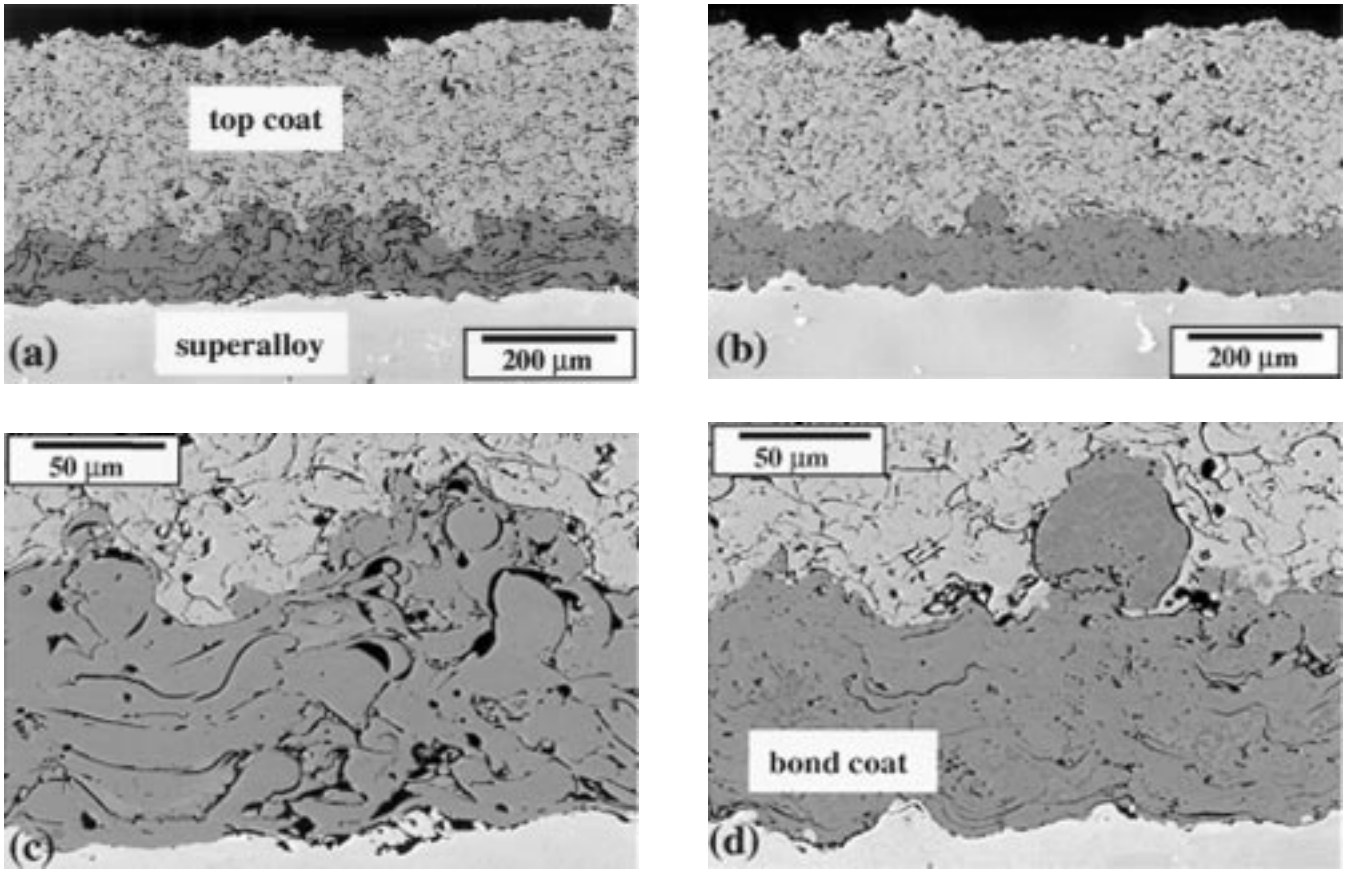

Fig. 1 BSE images of as-deposited TBCs showing (a) TBC with APS NiCrAl-1Y bond coat; (b) TBC with VPS NiCoCrAlYHfSi bond coat; (c) APS NiCrAl-1Y bond coat, with porosity and oxide inclusions (dark contrast phases); and (d) dense VPS NiCoCrAlYHfSi bond coat. The microstructure of (d) was representative of all VPS bond coats in the as-sprayed condition. The VPS bond coats experienced further densification after heat treatment at 1150 °C.

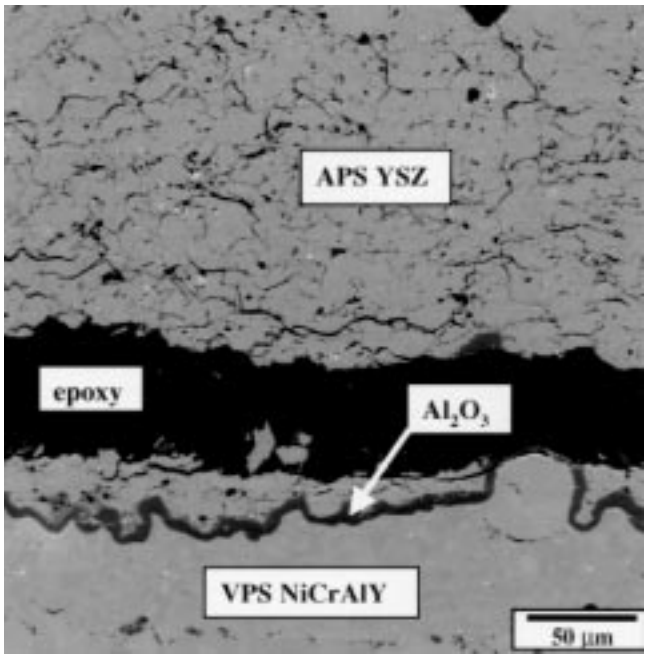

Fig. 2 SEM image of a typical cross section of a failed TBC (VPS NiCrAl-0.25Y, after 240 1 h cycles to 1150 °C). The failure mode of all TBCs in this study was fracture of the YSZ top coat parallel to the bond coat interface.

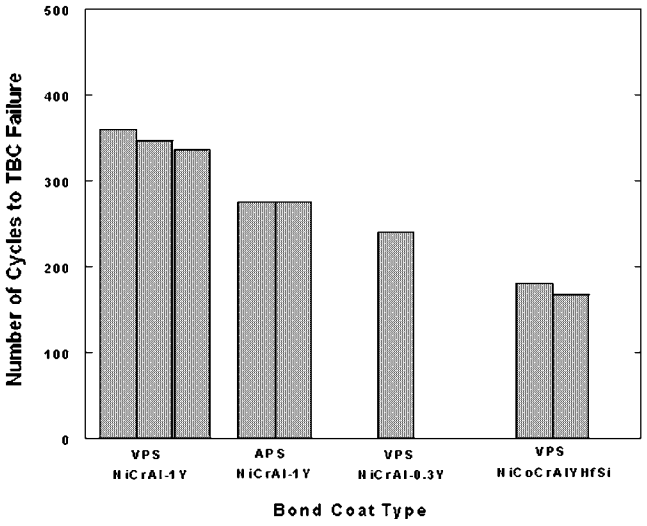

Fig. 3 Comparisons of the average lifetimes of plasma-sprayed TBCs with various bond coats on René N5 substrates, as determined by 1 h thermal cycles to 1150 °C. The mean TBC life and standard deviation are shown for each specimen type.

Since these specimens were coated on only one face, the weight gains of the coated specimens actually indicate the composite oxidation behavior of the plasma-sprayed MCrAlX surfaces and the René N5 surfaces. The coating weight gain values were not corrected for the actual MCrAlX surface areas (which were unknown because of the surface roughness) and, thus, are only valid for comparison purposes within this study (with these comparisons being limited by variations in bond coat surface roughness from specimen to specimen). The magnitude and rate of weight gain were greater for the TBC specimens than René N5, due to their greater surface area and inhibition of Al_2O_3 scale spallation from the MCrAlX-coated face by the APS YSZ. The cyclic oxidation rates of TBCs with VPS NiCrAl-1Y and NiCrAl-0.25Y bond coats were nearly identical, whereas TBCs with VPS NiCoCrAlYHfSi bond coats displayed a slightly higher rate after 100 cycles (Fig. 4).

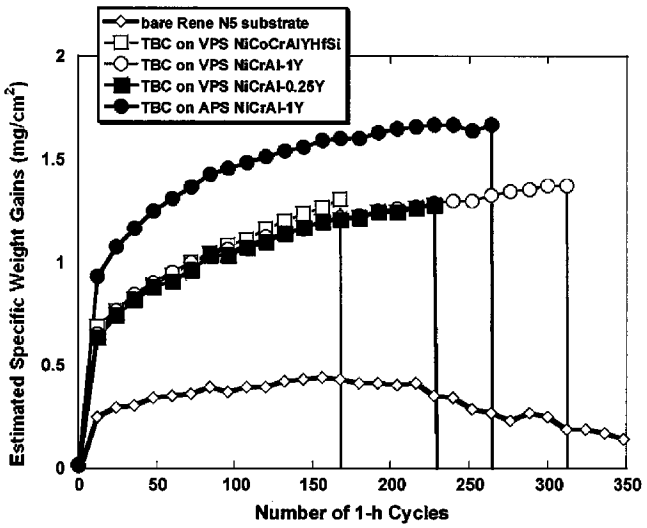

Fig. 4 Representative weight change curves from cyclic oxidation testing (at 1150 °C) of bare René N5 substrates and the four types of TBC specimens with various MCrAlX bond coats (coated with YSZ) on René N5 substrates. Note that only one face of the TBC specimens was coated.

3.3. Thermal Cycle Testing of Bare Bond Coats

René N5 substrates coated on one face with as-sprayed MCrAlX bond coats were also tested, to compare their relative scale adhesion behavior. Although there were no major differences in the cyclic oxidation behavior of the VPS MCrAlX bond coats (Fig. 5), there were subtle differences in the transient oxidation rates, the time to scale spallation, and the apparent rate of scale spallation. The VPS NiCoCrAlYHfSi displayed the lowest initial oxidation rate and maximum weight gain, as compared to VPS NiCrAl-1Y and NiCrAl-0.25Y. The points at which the weights of the VPS coatings (Fig. 5) begin to decrease can be considered the initiation of significant scale spallation. Significant scale spallation initiated at approximately 150 1 h cycles for bare René N5, 120 cycles for APS NiCrAl-1Y, 96 cycles for VPS NiCrAl-0.25Y, 72 cycles for VPS NiCrAl-1Y, and 60 cycles for VPS NiCoCrAlYHfSi. Furthermore, from comparison of the slopes of the curves after scale spallation initiated, René N5 displayed the most gradual rate of scale spallation (which appears to be only partially due to the lower surface area of the René N5), followed by VPS NiCrAl-1Y, VPS NiCoCrAlYHfSi, and then VPS NiCrAl-0.25Y. These comparisons suggest that Al_2O_3 scale adhesion to the René N5 surfaces during thermal cycling was superior to scale adhesion to the plasma-

sprayed MCrAlX bond coats. This result agrees with the relative oxidation behavior previously reported for cast NiCrAl and René N5.[19]

3.4. Electron Microprobe Analysis and Characterization of TBC Failure Mode

Bond coat compositions were measured before and after oxidation testing to investigate the effects of bond coat Al or Cr depletion (due to oxidation and substrate interdiffusion) on TBC durability. Table 4 compares the mean Ni, Co, Cr, and Al contents (averaged from the line scans across the bond coat thickness) of various bond coats in the as-deposited condition, after 100 1 h cycles and at TBC failure. The Al contents of the VPS bond coats were reduced after oxidation, but none were depleted below the Al content of the René N5 substrate (~6 wt.%), even at TBC failure. By comparison, the Al content of the APS NiCrAl-1Y (which provided superior TBC lifetimes as compared to VPS NiCoCrAlYHfSi) was 4.2 wt.% at TBC failure.

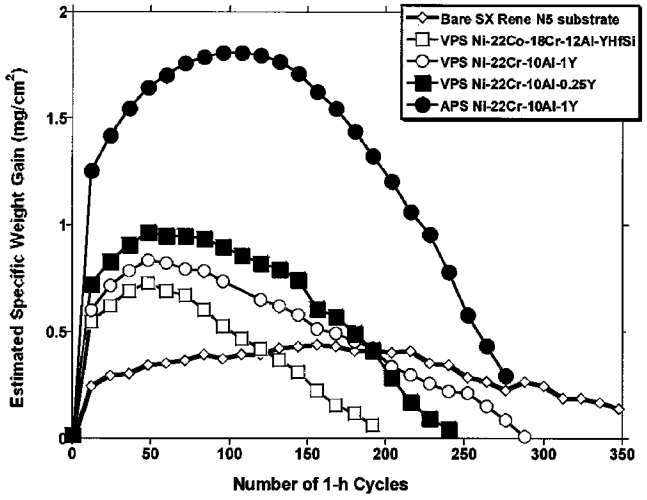

Fig. 5 Comparison of the weight changes during cyclic oxidation testing (1 h cycles at 1150 °C) of a René N5 substrate and various APS or VPS MCrAlX bond coats (with no YSZ top coat) on René N5 substrates. One specimen of each type was tested. Specimen weight losses are due to alumina scale spallation. Note that only one face of the substrates was coated with MCrAlX.

The Cr content of the as-deposited VPS NiCoCrAlYHfSi (~17 wt.%) was slightly lower than that of the VPS and APS NiCrAl-1Y (~22 wt.%). Note that the Cr content of each bond coat was reduced to ~14 wt.% at TBC failure, even though each TBC failed after significantly different test intervals (Fig. 3).

3.5. Thermal Expansion Measurements

Thermal expansion measurements of cast MCrAlX alloys confirmed that there were significant differences in the thermal expansion behavior of the NiCrAlY and NiCoCrAlY starting compositions. Figure 6 displays the mean coefficient of thermal expansion (CTE) versus temperature of the cast Ni-20Cr-10Al-0.3Y, cast Ni-22Co-18Cr-12.5Al-0.3Y, and René N5 over the temperature interval 25 to 1200 °C. The Ni-20Cr-10Al-Y alloy exhibited lower CTE values than NiCoCrAlY between 25 °C and approximately 1000 °C. However, the Ni-20Cr-10Al-Y experienced a high-temperature phase transformation, as indicated by a 25% increase in mean CTE over the temperature range 900 to 1030 °C. This transformation was reversible and has been previously reported for VPS Ni-22Cr-10Al-0.3Y.[5] The NiCoCrAlY did not exhibit an obvious phase transformation of this type. The René N5 superalloy exhibited the least thermal expansion over the entire range of testing. The mean CTE values of the Ni-20Cr-10Al-0.3Y, Ni-22Co-18Cr-12.5Al-0.3Y, and René N5 at 1150 °C were 20.3, 19.1, and 17.2×10^{-6}/°C, respectively.

3.6. Bond Coat Mechanical Properties

The Young's modulus and hardness values of the various bond coats versus time-at-temperature are plotted in Fig. 7(a) and (b), for selected bond coat compositions. The Young's modulus of VPS NiCoCrAlYHfSi and APS NiCrAl-1Y increased significantly after 100 1 h cycles, whereas that of the VPS NiCrAl-1Y increased only slightly. Previous work showed that this increase in E occurred during the first hour of heat treatment.[16]

The hardness values and behavior of the VPS NiCrAl-1Y and VPS NiCoCrAlYHfSi were similar, decreasing from 9.5 GPa in the as-sprayed condition to approximately 6.2 GPa after 100 1 h cycles at 1150 °C, thereafter remaining relatively constant to TBC failure (Fig. 7a). Note that a previous study determined that the sharp reduction in hardness of VPS NiCrAl-1Y occurred after only 1 h at 1150 °C.[16] The hardness of as-sprayed APS NiCrAl-1Y on René N5 was 4.9 GPa, but increased to 6.1 GPa

Table 4 Bond coat Ni, Co, Cr, and Al contents (wt. %)(a)

Bond coat	Substrate	Condition	Ni	Co	Cr	Al
APS NiCrAl-1Y	René N5	As-sprayed	67.6 ± 1.7	0.6 ± 0.1	21.9 ± 1.3	9.7 ± 1.1
APS NiCrAl-1Y	René N5	100 cycles	67.6 + 1.1	4.8 + 0.6	15.4 + 1.7	5.1 + 1.4
APS NiCrAl-1Y	René N5	276 cycles(b)	68.7 ± 1.0	5.8 ± 0.4	13.5 ± 2.2	4.6 ± 0.8
VPS NiCrAl-1Y	René N5	As-sprayed	62.9 ± 1.5	0.1 ± 0.1	21.7 ± 1.3	11.1 ± 0.6
VPS NiCrAl-1Y	René N5	100 cycles	67.7 ± 0.1	3.0 ± 0.1	17 ± 0.4	6.1 ± 0.1
VPS NiCrAl-1Y	René N5	360 cycles(b)	67.4 ± 2.0	4.2 ± 1.0	14.9 ± 2.1	6.0 ± 1.2
VPS NiCoCrAlX	René N5	As-sprayed	47.8 ± 0.7	21.4 ± 2.0	17.4 ± 1.4	13.8 ± 0.9
VPS NiCoCrAlX	René N5	100 cycles	58.0 ± 2.4	15.6 ± 3.6	12.7 ± 3.1	8.6 ± 3.5
VPS NiCoCrAlX	René N5	180 cycles(b)	58.3 ± 1.2	17.1 ± 0.6	13.9 ± 0.5	7.2 ± 0.4

(a) Each bond coat also contained Ta, W, Re, and Mo after oxidation testing. Bond coat compositions were calculated by averaging the line scans across the MCrAlX coating thickness. (b) Time corresponding to TBC failure (1 h cycles at 1150 °C)

after 100 1 h cycles and appeared to remain essentially constant to TBC failure (276 cycles). Thus, the room-temperature hardnesses of all bond coats on René N5 were essentially identical after 100 cycles.

3.7. Bond Coat Surface Roughness

There was little difference in the average surface roughness (R_a) of the as-sprayed bond coats (Table 5). However, there were slight differences in the standard deviations, which suggests that there may be differences in the morphology of the surface roughness, if not the magnitude. Characterization of TBC cross sections by SEM also suggested differences in the bond coat surface topologies. On a qualitative level, the surfaces of VPS NiCrAl-1Y appeared to be somewhat more irregular than the surfaces of VPS NiCoCrAlYHfSi and VPS NiCrAl-0.25Y, even though they were deposited with identical parameters and powder sizes.

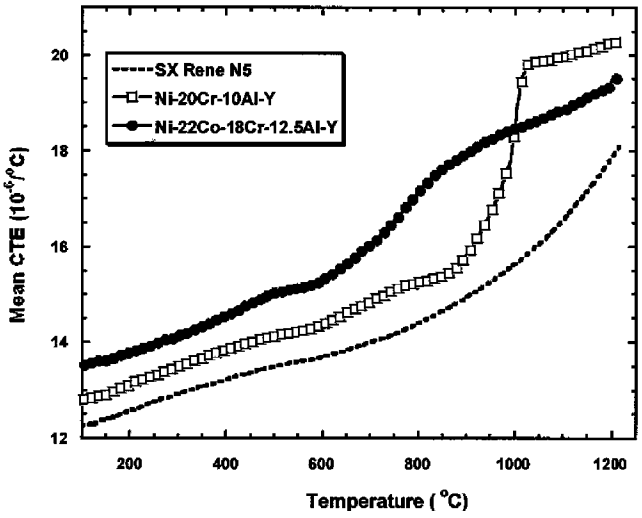

Fig. 6 Comparison of the mean CTE (25 to 1200 °C) of single-crystal Rene N5 to cast versions of the bond coat alloys used in this study (Ni-20Cr-10Al-Y and Ni-22Co-18Cr-12.5Al-Y).

4. Discussion

The carefully controlled TBC fabrication and testing conditions of this study revealed significant differences in the thermal cycle lifetimes of TBCs with various APS or VPS MCrAlX bond coats. The average lifetimes of all TBCs in this study were equal to or significantly better than the reported lifetimes of other plasma-sprayed TBCs in the literature,[1, 4, 8, 11, 17] so it can be concluded that the observed differences in TBC lifetime in this study were not due to substandard coating fabrication procedures. The present results suggest that the composition of the MCrAlX bond coat exerts a significant influence on the relative thermomechanical stability of plasma-sprayed TBCs during oxidation testing at an accelerated temperature, which is in agreement with previous studies.[1, 4, 11]

For the purposes of the following discussion, it is assumed that the plasma-sprayed YSZ top coats in this study were identical in structure and properties. Thus, the potential contributing factors to the observed variations in TBC durability included differences in (1) bond coat composition and subsequent variations with time-at-temperature, (2) bond coat mechanical properties and variations with time-at-temperature, (3) bond coat surface roughness, (4) bond coat oxidation behavior, (5) MCrAlX thermal expansion behavior, (6) bond coat surface topology, and (7) interfacial scale damage accumulation due to cyclic thermal stresses. Table 6 correlates the observed trends in these properties (and other related factors) with TBC lifetimes.

There was no apparent relationship between bond coat Al depletion and TBC durability. The hardness and Young's modulus of the various bond coats in this study were very similar after 100 1 h cycles (Fig. 7a and b). The reasons for the changes in APS and VPS bond coat hardness after heat treatment are discussed elsewhere.[16] Note that these ambient temperature mechanical properties measurements do not necessarily provide an indicator of the relative high-temperature properties of the various bond coats. It

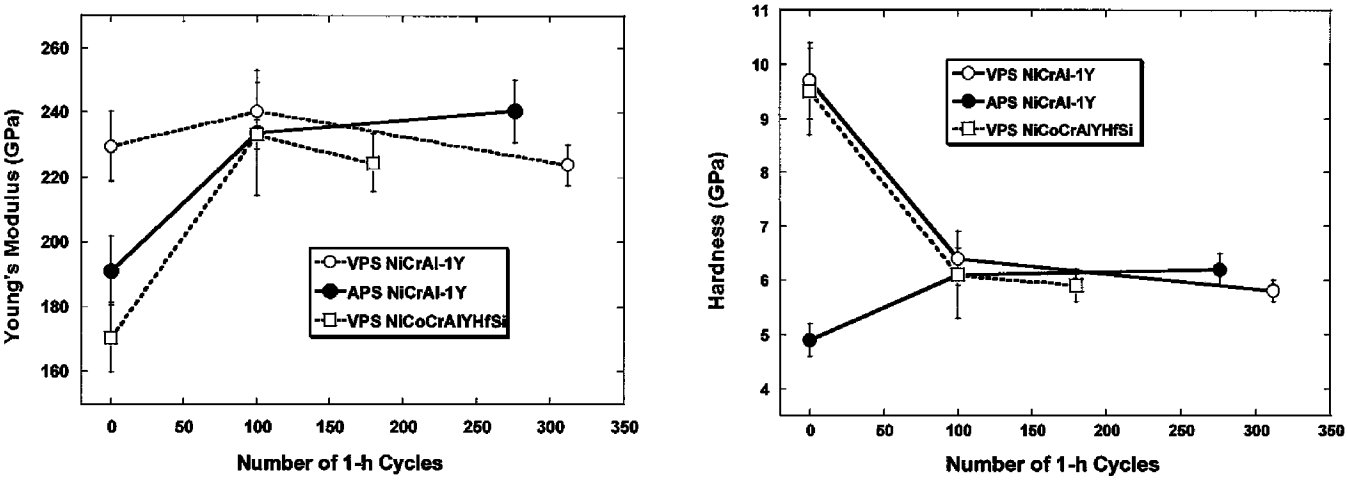

Fig. 7 Mechanical properties of the various MCrAlX bond coats (on Rene N5 substrates) with respect to number of cycles to 1150 °C, as measured by mechanical properties microprobe. (**a**) MCrAlX Young's modulus and (**b**) MCrAlX hardness. The properties of all MCrAlX bond coats were very similar after heat treatment.

was possible that subtle differences in bond coat surface topology, unrelated to R_a, may have influenced TBC performance.

4.1 Cyclic Oxidation Behavior

From review of the literature, it was anticipated that TBCs with VPS bond coats would have significantly longer thermal cycle lifetimes than TBCs with APS bond coats, primarily due to the superior oxidation resistance of VPS bond coats.[1, 2, 3] It was also expected that the durability of TBCs with VPS NiCoCrAlYHfSi bond coats would be equal to or superior to that of TBCs with NiCrAlY-type bond coats, especially since the NiCoCrAlY-type alloys do not undergo a significant volumetric increase due to high-temperature phase transformation (Fig. 6). Contrary to these expectations, the average lifetimes of TBCs with VPS NiCrAl-1Y bond coats were only 20% greater than those of TBCs with APS NiCrAl-1Y bond coats, and were twice those of TBCs with VPS NiCoCrAlYHfSi bond coats. Even more surprising was the fact that APS NiCrAl-1Y bond coats yielded TBC lifetimes that were a factor of 1.6 greater than those of TBCs with VPS NiCoCrAlYHfSi bond coats (Fig. 3).

The results described here suggest that the significant variations in TBC lifetimes may be associated with subtle differences in the oxidation behavior of the NiCrAlY and NiCoCrAlYHfSi bond coats. The oxidation rates of TBCs with VPS NiCoCrAlYHfSi bond coats were slightly higher than those with VPS NiCrAlY (Fig. 4), which could be due to small differences in oxide scale growth rates or a larger NiCoCrAlYHfSi coating surface area. However, SEM analysis of metallographic cross sections suggested a slightly more irregular surface (and a potentially larger surface area) on the VPS NiCrAl-1Y bond coats.

Alternatively, the slight increase in TBC cyclic oxidation rate could be an indication that greater amounts of cracking and delamination were occurring in the interfacial Al_2O_3 scales on VPS NiCoCrAlYHfSi. Previous studies have reported significant localized damage in the interfacial Al_2O_3 scales after thermal cycling of APS TBCs.[7,8,9,15] Since the YSZ top coat prevents scale spallation, an increase in the susceptibility to scale damage would accelerate the apparent TBC cyclic oxidation rate due to rapid oxide reformation beneath the cracked or delaminated interfacial Al_2O_3 scales. This would be the case even if the intrinsic isothermal oxidation rates of NiCrAlY and NiCoCrAlYHfSi were similar. Analysis of metallographic cross sections of cycled TBCs by SEM confirmed that varying amounts of localized cracking, delamination, and reformation of the interfacial Al_2O_3 scales had occurred on all bond coats after 100 cycles, as illustrated in Fig. 8(a) and (b). Further research will be required to effectively quantify the relative amounts and frequency of interfacial scale damage, as well as their potential influence on TBC durability.

Comparison of the thermal cycle behavior of the bare MCrAlX coatings provides additional insight into the relative scale adhesion behavior of the various bond coats and supports the presumption that differences in APS TBC lifetimes might have been related to bond coat scale adhesion behavior. The TBC durability generally decreased as the time to initiation of scale spallation decreased or as the rate of scale spallation increased (Fig. 5). Coincidentally, each type of TBC typically failed at or near the number of cycles that corresponded to the time at which their respective bond coat specimen spalled to its original weight, as illustrated in Fig. 9. This observation implies that the relative times to TBC failure may have been

Table 5 Bond coat surface roughness

Bond coat type	APS NiCrAl-1Y	VPS NiCrAl-1Y	VPS NiCrAl-0.25Y	VPS NiCoCrAlYHfSi
R_a (μm)	10.6	11.8	10.2	11.8
Standard Deviation	0.3	0.5	1.3	1.1

R_a is the arithmetical mean deviation of all roughness profile values (from the mean line).

Table 6 Qualitative comparisons of the apparent effects of various coating properties on trends in TBC lifetimes

Property	Significant effect on TBC life	Potential effect on TBC life	No effect on TBC life
Bond coat starting composition	X		
MCrAlX CTE below 1000 °C	X		
Time to initiation of scale spallation(a)	X		
Apparent scale spallation rate(a)	X		
Bond coat Cr content		X	
Bond coat surface topology		X	
TBC cyclic oxidation rate		X	
Internal oxidation of the APS bond coat		X	
Bond coat Youngs modulus(b)			X
Bond coat hardness(b)			X
Bond coat Al content			X
MCrAlX CTE at 1150 °C			X
Average bond coat surface roughness			X
Bond coat cyclic oxidation rate			X

(a) Bare bond coat. (b) At 25 °C

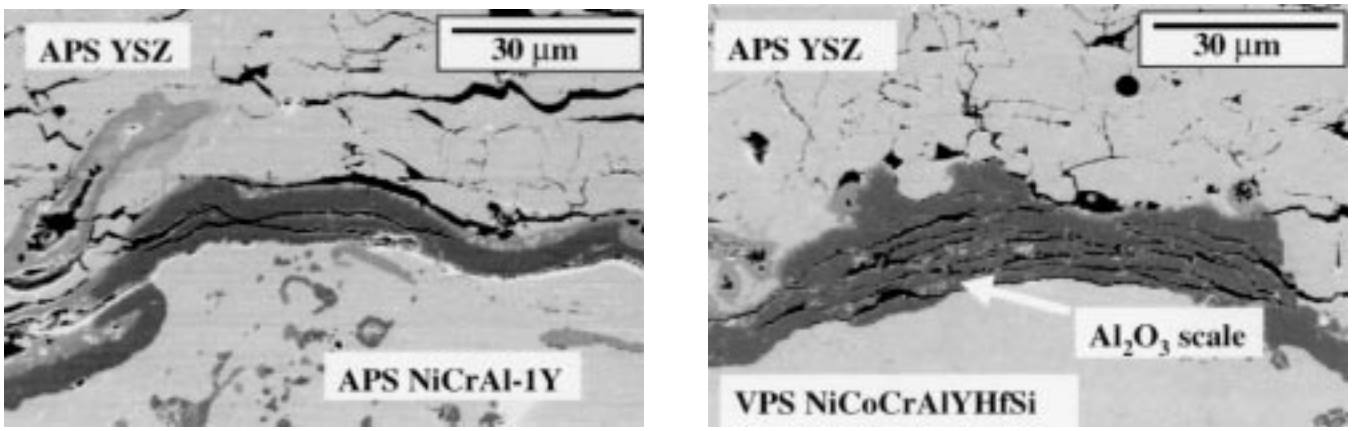

Fig. 8 Secondary electron images of TBC cross sections after thermal cycling, showing the presence of localized damage in the Al_2O_3 interface scales after 100 cycles: (a) TBC with APS NiCrAl-1Y bond coat and (b) TBC with VPS NiCoCrAlYHfSi bond coat. Although there was significant scale damage (in the form of cracking and multilayering) in localized regions, scale cracking was not visible over the majority of the interface.

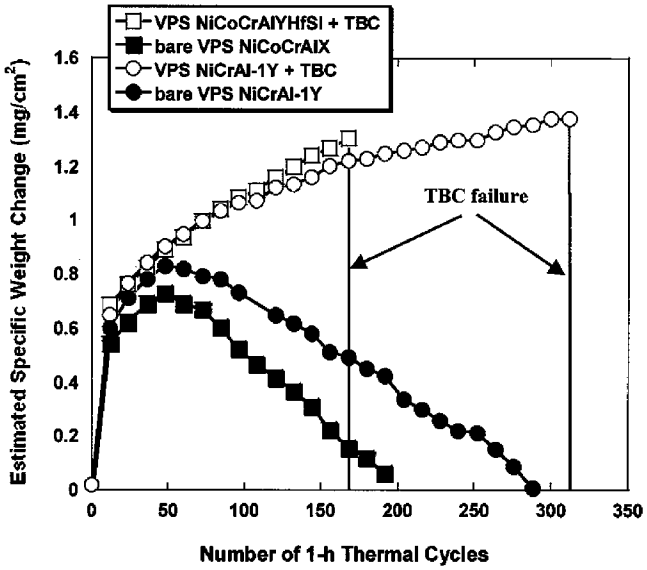

Fig. 9 Comparison of TBC and bond coat oxidation behavior at 1150 °C. Note that TBC failure occurs near the time at which the bond coat specimen weight decreases to the original specimen weight (due to scale spallation). This behavior was typical of all four bond coat compositions on René N5.

influenced by some critical amount of interfacial Al_2O_3 damage accumulation.

Although it is well known that TBC degradation is accelerated under oxidizing conditions,[20] and that TBC lifetimes are dependent on both the number of thermal cycles and the time-at-temperature, there is no clear understanding of the influence of bond coat composition or oxidation behavior (*i.e.*, scale growth rates and scale adhesion). Brindley and Miller reported that the intrinsic isothermal oxidation rates of various NiCrAlY bond coats were not necessarily an indicator of relative TBC performance.[4] Other investigations have suggested that the relative durability of plasma-sprayed TBCs on various bond coats was strongly influenced by bond coat creep resistance[1, 11] or the interaction of bond coat stress relaxation behavior with bond coat CTE behavior.[11] Bartlett and Dal Maschio suggested that failure of plasma-sprayed TBCs is facilitated by cracks that form in the brittle Al_2O_3 scales and then propagate into the adjacent YSZ layer.[8] However, this conclusion does not agree with the observations of other studies, which reported that the critical YSZ cracks that caused TBC spallation did not initiate in the Al_2O_3 scale.[7, 16] Thus, the role of interfacial Al_2O_3 scale cracking within the TBC damage accumulation process is still unclear.

4.2 Thermal Expansion Behavior

The CTE curves for cast Ni-20Cr-Al-1Y in Fig. 6 were similar to those reported in Ref 5 for monolithic VPS Ni-22Cr-10Al-0.3Y. Thus, it was concluded that the CTE results for the cast MCrAlX alloys are representative of bond coat behavior. The magnitude of the residual stresses generated in the Al_2O_3 and YSZ layers during cooling should be proportional to the difference in metal and ceramic CTE values, with all other factors constant. Thus, for identical peak temperatures, the bond coat with a lower CTE provides lower residual stress in the ceramic layers after cooling to ambient temperature (assuming similar high-temperature mechanical properties), which should result in both improved oxide scale adhesion and increased TBC durability. The lower CTE values of René N5 (Fig. 6) agree with its excellent Al_2O_3 scale adhesion, as compared to the MCrAlX alloys (Fig. 5).

The thermal stress, $\sigma_{\Delta T}$, in the thin YSZ top coats can be approximated (assuming a biaxial stress state) by

$$\sigma_{\Delta T} = \Delta T \Delta \alpha E / (1 - \mu) \quad \text{(Eq 1)}$$

where ΔT is the difference between ambient temperature and peak temperature, $\Delta\alpha$ is the difference in mean CTE between the ceramic and metal layers, E is the Young's modulus of the YSZ top coat, and μ is the Poisson ratio of the YSZ top coat.[20] The values of E, α, and μ for APS YSZ are approximately 50 GPa,[20] 10×10^{-6} °C^{-1},[5, 7] and 0.25 (as estimated in Ref 20), respectively. Based on the 1150 °C CTE values in Fig. 6, a ΔT of 1125 °C would induce biaxial thermal stresses of approximately −773 and −683 MPa for APS YSZ top coats with Ni-20Cr-10Al-Y and Ni-22Co-18Cr-12.5Al-Y bond coats, respectively. This corre-

sponds to ~13% increase in residual thermal stress for TBCs on NiCrAlY compared to NiCoCrAlYHfSi, which does not explain the observed doubling in TBC durability on VPS NiCrAl-1Y.

The above comparison suggests that bond coat CTE behavior at the peak temperature (1150 °C) was not a dominant factor in determining the relative durability of specific TBC systems. However, if one considers that rapid stress relaxation of MCrAlX alloys typically initiates in the 600 to 800 °C range,[5, 11, 13] then cooling stresses generated above the ductile-to-brittle transition temperature of the bond coat are eliminated.[11] Furthermore, note that in Fig. 6 the mean CTE of NiCrAlY is significantly lower than that of NiCoCrAlY below ~900 °C. Thus, it is possible that the relative levels of residual stress in the overlying ceramic layers are not determined by the expansion behavior from the peak temperature, but are instead determined by the relative bond coat thermal expansion behavior below an intermediate temperature, as has been suggested previously.[11]

The NiCrAlY and NiCoCrAlY mean CTE values at 800 °C were measured as 15.2 and 17.1×10^{-6} °C^{-1}, respectively (Fig. 6). Using a ΔT of 775 °C, and assuming MCrAlX stress relaxation above 800 °C, Eq 1 estimates a 38% increase in biaxial residual stress for TBCs with NiCoCrAlY bond coats (which does not account for differences in bond coat stress relaxation or stress intensification due to oxidation and the irregular bond coat surface). This estimation agrees with the observed trends in TBC durability; *i.e.*, lower residual stress yields longer TBC lifetimes. These results support Brindley's theory that the YSZ residual stresses for a specific TBC system are determined by the combined effects of the bond coat stress relaxation behavior and the path of the bond coat CTE curve below the relaxation temperature.[11]

From the perspective of CTE behavior, it can be asked why the average lifetimes of TBCs with VPS NiCrAl-1Y bond coats were consistently better than those of TBCs with APS NiCrAl-1Y, since the only significant difference in the as-deposited coatings was the bond coat fabrication process. It could be argued that APS NiCrAl-lY might provide a slight decrease in YSZ residual stress, since its effective CTE is likely reduced by the significant amounts of dispersed internal oxides. The reason for the decreased TBC durability was not clear, but it is possible that the APS NiCrAl-1Y experienced a slight volume increase due to oxidation along internal porosity, which may have accelerated TBC failure by increasing out-of-plane YSZ tensile stresses. The relative lifetimes may have also been affected by subtle differences in bond coat surface morphology or scale adhesion behavior.

It is also probable that the thermal expansion behavior of each bond coat is not constant with time at temperature, since the bond coat composition changes significantly during high-temperature exposure (Table 4). Thus, in order to facilitate more accurate stress models, there is a need to determine the CTE behavior and the time- and temperature-dependent mechanical properties of specific bond coats (on specific substrate alloys).

Bond coat scale adhesion and CTE behavior below 900 °C were the properties that most closely correlated to the observed trends in TBC durability (Table 6). It is not clear which, if either, of their related degradation mechanisms resulted in the significant variations in TBC lifetimes in this investigation. With regard to the influence of CTE, analysis is complicated by a lack of information on the relative creep behavior and time-dependent thermal expansion behavior of NiCrAlY and NiCoCrAlYHfSi. The superior TBC lifetimes on NiCrAl-1Y as compared to NiCrAl-0.3Y (Fig. 3), and the fact that the scale spallation rate on NiCrAl-0.25Y was higher than that of NiCrAl-1Y (Fig. 4), support the hypothesis that scale adhesion behavior may have been a significant contributor to TBC degradation (since the CTE of these two bond coats should have been effectively identical). However, to our knowledge, there have been no previous studies comparing the cyclic oxidation behavior of various bond coats with their relative plasma-sprayed TBC lifetimes. Additional confirmation of the oxidation-related trends observed in this investigation is needed.

5. Summary

- Plasma-sprayed TBCs with APS and VPS Ni-22Cr-10Al-1Y bond coats exhibited significantly better durability than TBCs with VPS Ni-22Co-18Cr-12.5Al-YHfSi bond coats.
- Although the mean CTE of cast Ni-20Cr-10Al-Y was higher than that of cast NiCoCrAlY at 1150 °C, NiCrAlY bond coats provided superior TBC lifetimes. It was concluded that the path of the CTE curve at intermediate temperatures exerted a more significant influence on TBC durability (due to the effects of bond coat stress relaxation), since the mean CTE of NiCrAlY was less than that of NiCoCrAlY below 1000 °C. This result agrees with that of previous investigations.
- Bond coat compositions with superior scale adhesion (*i.e.*, longer times to initiation of scale spallation and lower rates of scale spallation) provided significantly better TBC lifetimes. This result suggests that, for plasma-sprayed TBCs with good oxidation resistance, the rate of damage accumulation in the interfacial Al_2O_3 scale may influence relative TBC durability.
- There was no correlation between APS TBC lifetime and bond coat hardness (at 25 °C), Young's modulus (at 25 °C) Al depletion rate, and average surface roughness.
- The lifetimes of TBCs with APS MCrAlX bond coats were similar to or superior to those of TBCs with VPS MCrAlX bond coats, which suggests that APS bond coats, which are more cost-effective, may be competitive with VPS bond coats for some TBC applications.
- The results of this study emphasize the importance of thoroughly determining the oxidation behavior and the temperature- and time-dependent physical and mechanical properties of various bond coat systems prior to attempting to fully define and model the dominant degradation mechanisms in plasma-sprayed TBCs.

Acknowledgments

The authors would like to thank S. Walston of G.E. Aircraft Engines for providing the René N5 substrate materials; G. Bancke and Professor C. Berndt of the Thermal Spray Lab at SUNY for plasma spraying of all coatings; B. Pint and I. Wright at ORNL for the cast MCrAlX alloys; T. Geer at ORNL for metallography; and T. Besmann, M. Brady, and I. Wright at ORNL for helpful reviews. Research sponsored by the U.S. Department of Energy, Assistant Secretary for Energy Efficiency and Renewable Energy, Office of Industrial Technologies, Advanced Turbine Systems

Materials Program, under Contract No. DE-AC05-96OR22464 with Lockheed Martin Energy Research Corporation.

References

1. D.J. Wortman, B.A. Nagaraj, and E.C. Duderstadt: *Mater. Sci. Eng.*, 1989, vol. A121, pp. 433–40.
2. S.M. Meier, D. K. Gupta, and K.D. Sheffler: *JOM*, 1991, vol. 43 (3), pp. 50–53.
3. R.A. Miller: *J. Thermal Spray Technol.*, 1997, vol. 6 (1), pp. 35–42.
4. W.J. Brindley and R.A. Miller: *Surf. Coating Technol.*, 1990, vol. 43–44, pp. 446–57.
5. R.V. Hillery, B.H. Pilsner, R.L. McKnight, T.S. Cook, and M.S. Hartle: "Thermal Barrier Coating Life Prediction Model Development," Final Report, NASA CR 180807, National Aeronautics and Space Administration, Washington, DC, Nov. 1988.
6. B.A. Pint, I.G. Wright, W.Y. Lee, Y. Zhang, K. Pruβner, and K.B. Alexander: *Mater. Sci. Eng.*, 1998, vol. A245, pp. 201–11.
7. J.T. DeMasi-Marcin, K.D. Sheffler, and S. Bose: *J. Eng. Gas Turbines Power*, 1990, vol. 112, pp. 521–26.
8. A.H. Bartlett and R. Dal Maschio: *J. Am. Ceram. Soc.*, 1995, vol. 78 (4), pp. 1018–24.
9. J.A. Haynes, M.K. Ferber, E.D. Rigney, and W.D. Porter: *Surf. Coating Technol.*, 1996, vol. 86–87, pp. 102–08.
10. M.J. Lance, J.A. Haynes, W.R. Cannon, and M.K. Ferber: in *Ceramic Transactions: Nondestructive Evaluation of Ceramics*, C.H. Schilling and J.N. Gray, eds., American Ceramic Society, Westerville, OH, 1998, vol. 89, pp. 229–37.
11. W.J. Brindley: *J. Thermal Spray Technol.*, 1997, vol. 6 (1), pp. 85–90.
12. D.M. Nissley: *J. Thermal Spray Technol.*, 1997, vol. 6 (1), pp. 91–98.
13. W.J. Brindley and J.D. Whittenberger: *Mater. Sci. Eng.*, 1993, vol. A163, pp. 33–41.
14. J.T. DeMasi, K.D. Sheffler, and M.Ortiz: "Thermal Barrier Coating Life Prediction Model Development, Phase 1," Final Report, NASA CR 182230, National Aeronautics and Space Administration, Washington, DC, Dec. 1989.
15. J.A. Haynes, M.K. Ferber, and E.D. Rigney: *Oxid. Met.*, vol. 52, Nos.1/2, 1999, pp. 31–76.
16. J.A. Haynes, M.K. Ferber, W.D. Porter, E.D. Rigney: *Materials at High Temperatures*, 1999, vol. 16(2), pp. 49–69.
17. B.C. Wu, E. Chang, C.H. Chao, and M.L. Tsai: *J. Mater. Sci.*, 1990, vol. 25, pp. 1112–119.
18. P.F. Tortorelli, S.R.J. Saunders, G. Shafirstein, and D.J. Hall: *Mater. High Temp.*, 1994, vol. 12 (2–3), pp. 95–101.
19. B.A. Pint and I.G. Wright: in *High Temperature Corrosion and Materials Chemistry*, Electrochemical Society Proc. P.Y. Hou, M.J. McNallan, R. Oltra, E.J. Opila, and D.A. Shores, eds., 1998, vol. 98–99, pp. 263–74.
20. R.A. Miller and C.E. Lowell: *Thin Solid Films*, 1982, vol. 95, pp. 265–73.